Available online at www.sciencedirect.com
ScienceDirect
Desalination 242 (2009) 70–83
DESALINATION
www.elsevier.com/locate/desal

Effect of ultrafiltration on the mass-transfer efficiency improvement in a parallel-plate countercurrent dialysis system

Jr-Wei Tu[a], Chii-Dong Ho[a]*, Ching-Jung Chuang[b]

[a]*Department of Chemical and Materials Engineering, Tamkang University, Tamsui, Taipei, Taiwan, ROC*
Tel. +886 (2) 2621-5656 ext. 2724; Fax +886 (2) 26209887; email: cdho@mail.tku.edu.tw
[b]*R&D Center for Membrane Technology and Department of Chemical Engineering, Chung Yuan Christian University, Taoyuan, Taiwan, ROC*

Received 18 January 2007; accepted revised 20 March 2008

Abstract

A mathematical model for the mass transfer in a parallel plate countercurrent dialysis system coupled with ultrafiltration operation was developed theoretically and experimentally in this study. The analytical solution was obtained using the Frobenius series method. The influences of retentate and dialysate phase flow rates, ultrafiltration flux and solute sieving factor on the outlet concentrations and mass transfer rate were also represented graphically in this study. The analytical predictions show that the introduction of ultrafiltration effects in a dialysis system leads to considerable enhancement of the separation efficiency as compared to that in a pure dialysis system without ultrafiltration. An experimental apparatus was also set up to confirm the accuracy of the proposed mathematical model, and the comparisons show that a qualitative agreement between the theoretical predictions and experimental results was achieved.

Keywords: Mass-transfer efficiency improvement; Dialysis; Ultrafiltration; Countercurrent

1. Introduction

Membrane-based separation processes have been widely used in concentration or purification processes, as referred to the membrane contactors [1], such as solvent extraction [2–4], gas absorption [5–7], ion exchange [8,9] and membrane distillation [10,11]. Membrane dialysis is one of the membrane contactors and the solutes are transported from one side of the membrane (retentate phase) to the other side (dialysate phase) by diffusion. Different from the other membrane contactors, the solvent may also transport through the membrane in a membrane dialysis process. The most famous application of membrane dialysis is hemodialysis (artificial kidney) which removes waste metabolic end products from the human body [12,13].

*Corresponding author.

0011-9164/09/$– See front matter
doi:10.1016/j.desal.2008.03.032

To simplify the mass transfer problem, the early analysis of membrane dialysis [14–16] considered only the concentration variations in the retentate phase and assumed that the dialysate phase concentration was constant and no solvent passed through the membrane. In fact, the dialysate phase concentration would not be constant and the solvent unavoidably transports through the membrane in a membrane dialysis process. Cooney et al. [17] took account of the effect of the diaysate phase concentration variations on the mass transfer phenomena between retentate and dialysate phases in the parallel-plate and cylindrical tube hemodialyzers. The mass transfer of the higher [18] or lower fiber packing density hollow fiber dialyzers [19] with ignoring the ultrafiltration effect was also investigated. Popovich et al. [20] studied the effect of ultrafiltration on the mass transfer in a flat-plate dialyzer by assuming a zero solute concentration in the dialysate phase. Application of ultrafiltration operation in a membrane dialyzer can readily improve the mass transfer efficiency by transporting the solute in diffusion and convection simultaneously. Henderson [21] and Leber et al. [22] showed that high efficiency hemodialysis with ultrafiltration can reduce the treatment time and is tolerated by patients. Jagannathan and Shettigar [23] demonstrated that the ultrafiltration effect leads to the improvement of the device performance of a fiber hemodialyzer with varying dialysate concentration. Abbas and Tyagi [24,25] obtained an analytical solution for the retentate concentration profile in hollow fiber dialyzers and circular conduit dialyzers coupled with ultrafiltration by assuming the constant ultrafiltration flux and dialysate concentration. Yeh et al. [26,27] analyzed mass transfer in a cross-flow parallel-plate dialyzer coupled with ultrafiltration by using the perturbation method.

The purposes of the present study are firstly to develop the mathematical formulation of a parallel-plate countercurrent dialysis system, and then to obtain analytical solutions by using the Frobenius series method, and finally to investigate ultrafiltration effects on the mass-transfer efficiency improvement in such dialysis-and-ultrafiltration system theoretically and experimentally. The effects of retentate phase flow rate, dialysate phase flow rate, ultrafiltration flux and membrane sieving coefficient on the mass transfer rate are also delineated in this study.

2. Mass transfer model

Fig. 1 shows a flat-plate membrane dialyzer with length L and width W. The retentate fluid flows into the upper channel with volumetric flow rate $Q_{R,i}$ and concentration $C_{R,i}$ at $x = 0$ while the dialysate fluid flows into the bottom channel with volumetric flow rate $Q_{D,i}$ and concentration $C_{D,i}$ at $x = L$. A transmembrane pressure is applied to the dialyser resulting in an average ultrafiltration flux $\bar{V}_m$ as shown in Fig. 1. As referred to in [28] and [29], in a countercurrent operation, the transmembrane pressure and ultrafiltration flux will decrease along the conduit length. However, in order to simplify the mathematical model, the average transmembrane pressure and ultrafiltration flux were used in the calculation procedure in this study. The conservation equations are developed using the following assumptions: (1) the fluids flow in parallel in both retentate and dialysis phases; (2) the fluids physical properties are constant; (3) the overall mass transfer coefficient and the membrane sieve coefficient of solute are constant. With the aid of those assumptions, the mass balance equations for the solute in both phases were derived in the form

$$-\frac{dQ_R}{Wdx} = -\frac{dQ_D}{Wdx} = \bar{V}_m \tag{1}$$

$$-\frac{d\left(Q_R C_R\right)}{Wdx} = -\frac{d\left(Q_D C_D\right)}{Wdx} = K\left(C_R - C_D\right) + \bar{V}_m \bar{\theta} C_R \tag{2}$$

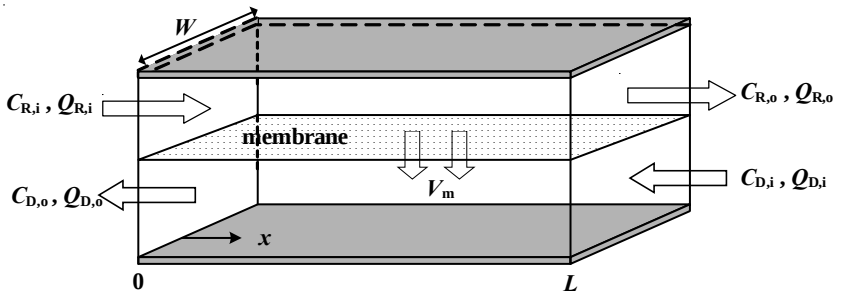

Fig. 1. The flat-plate countercurrent membrane dialyser.

where K is the overall mass transfer coefficient of the solute and $\bar{\theta}$ is the average membrane sieving coefficient in which $\bar{\theta} = 0$ means that the solute can freely pass through the membrane while $\bar{\theta}$ is less than unity, denoting that the solutes are partially rejected by the membrane. The subscripts R and D refer to the retentate and dialysate phases, respectively. The boundary conditions of Eq. (1) are

$$x = 0,\ Q_R = Q_{R,i} \tag{3}$$

$$x = L,\ Q_D = Q_{D,i} \tag{4}$$

The flow rate in both phases along with the conduit length can be obtained by integrating Eq. (1) with boundary conditions, Eqs. (3) and (4):

$$Q_R = Q_{R,i} - \int_0^x W\bar{V}_m dx = Q_{R,i} - W\bar{V}_m x \tag{5}$$

$$Q_D = Q_{D,i} - \int_L^x W\bar{V}_m dx = Q_{D,i} + W\bar{V}_m (L - x) \tag{6}$$

Substituting Eqs. (5) and (6) into Eq. (2) results in:

$$-\frac{dC_R}{dx} = \frac{W}{Q_{R,i} - W\bar{V}_m x}\left\{C_R\left[K + \bar{V}_m\left(\bar{\theta} - 1\right)\right] - KC_D\right\} \tag{7}$$

$$-\frac{dC_D}{dx} = \frac{W}{Q_{D,i} + W\bar{V}_m (L - x)}\left[C_R\left(K + \bar{V}_m\bar{\theta}\right) - C_D\left(K + \bar{V}_m\right)\right] \tag{8}$$

With the aid of the following dimensionless groups

$$\begin{aligned} &\xi = x/L,\ \zeta_R = C_R/C_{R,i},\ \zeta_D = C_D/C_{R,i},\\ &\varepsilon = C_{D,i}/C_{R,i},\ a = LWK/Q_{R,i},\\ &b = LWK/Q_{D,i},\ \bar{\psi} = \bar{V}_m/K \end{aligned} \tag{9}$$

Eqs. (7) and (8) can be rewritten in the dimensionless form as

$$-\frac{d\zeta_R}{d\xi} = \frac{a}{1 - a\bar{\psi}\xi}\left\{\left[1 + \bar{\psi}\left(\bar{\theta} - 1\right)\right]\zeta_R - \zeta_D\right\} \tag{10}$$

$$-\frac{d\zeta_D}{d\xi} = \frac{b}{1 + b\bar{\psi}(1 - \xi)}\left[\zeta_R\left(1 + \bar{\psi}\bar{\theta}\right) - \zeta_D\left(1 + \bar{\psi}\right)\right] \tag{11}$$

The corresponding dimensionless boundary conditions of Eqs. (10) and (11) are

$$\xi = 0,\ \zeta_R = 1 \tag{12}$$

$$\xi = 1,\ \zeta_D = \varepsilon \tag{13}$$

Rearranging Eq. (10) gives

$$\zeta_D = \left(\frac{1}{a} - \overline{\psi}\xi\right)\frac{d\zeta_R}{d\xi} + \left[1 + \overline{\psi}\left(\overline{\theta} - 1\right)\right]\zeta_R \tag{14}$$

and differentiation of Eq. (14) with respect to ξ is

$$\frac{d\zeta_D}{d\xi} = \left(\frac{1}{a} - \overline{\psi}\xi\right)\frac{d^2\zeta_R}{d\xi^2} + \left[1 + \overline{\psi}\left(\overline{\theta} - 2\right)\right]\frac{d\zeta_R}{d\xi} \tag{15}$$

Then substituting Eqs. (14) and (15) into Eq. (11) yields

$$\left(A_2\xi^2 + A_1\xi + A_0\right)\frac{d^2\zeta_R}{d\xi^2} + \left(B_1\xi + B_0\right)\frac{d\zeta_R}{d\xi} + C_0\zeta_R = 0 \tag{16}$$

where

$$A_2 = -\overline{\psi}^2,\ A_1 = \overline{\psi}\left(\frac{1}{a} + \frac{1}{b} + \overline{\psi}\right),\ A_0 = -\frac{1}{ab} - \frac{\overline{\psi}}{a},\ B_1 = \overline{\psi}^2\left(\overline{\theta} - 3\right), \tag{17}$$

$$B_0 = \frac{1}{a} - \frac{1}{b} + \overline{\psi}\left(\frac{1}{a} - \frac{\left(\overline{\theta} - 2\right)}{b} - 1\right) - \overline{\psi}^2\left(\overline{\theta} - 2\right),$$

$$C_0 = \left(\overline{\theta} - 1\right)\overline{\psi}^2$$

A power series method was used to solve Eq. (16) and ζ_R can be expanded in the form:

$$\zeta_E = \sum_{k=0}^{\infty} d_k \xi^{k+\lambda} \tag{18}$$

Substituting Eq. (18) into the Eq. (16) gives

$$\begin{aligned} &A_0\lambda\left(\lambda - 1\right)d_0\xi^{\lambda-2} + \left\{\left[A_1\lambda\left(\lambda - 1\right) + B_0\lambda\right]d_0 + \left[A_0\lambda\left(\lambda + 1\right)d_1\right]\right\}\xi^{\lambda-1} + \sum_{k=0}^{\infty}\left\{\left[A_2\left(k + \lambda\right)\left(k + \lambda - 1\right) + B_1\left(k + \lambda\right) + C_0\right]d_k\right. \\ &\left. + \left[A_1\left(k + \lambda + 1\right)\left(k + \lambda\right) + B_0\left(k + \lambda + 1\right)\right]d_{k+1} + \left[A_0\left(k + \lambda + 2\right)\left(k + \lambda + 1\right)\right]d_{k+2}\right\}\xi^{k+\lambda} = 0 \end{aligned} \tag{19}$$

Applying the Frobenius series method to Eq. (18) leads to:

$$\zeta_R = \sum_{k=0}^{\infty} d_{a,k}\xi^{k+1} + \sum_{k=0}^{\infty} d_{b,k}\xi^{k} \tag{20}$$

where

$$d_{a,1} = -\left(\frac{B_0}{2A_0}\right)d_{a,0},\ d_{a,k} = -\frac{\left[A_2\left(k-1\right)\left(k-2\right) + B_1\left(k-1\right) + C_0\right]d_{a,k-2} + \left[A_1 k\left(k-1\right) + B_0 k\right]d_{a,k-1}}{A_0\left(k+1\right)k},\quad k \geq 2 \tag{21}$$

and

$$d_{b.1} = -\frac{\left[B_0 - A_1\right]}{A_0}d_{b,0},$$

$$d_{b,k} = -\frac{\left[A_1\left(k-1\right)\left(k-2\right) + B_0\left(k-1\right)\right]d_{b,k-1} + \left[A_2\left(k-2\right)\left(k-3\right) + B_1\left(k-2\right) + C_0\right]d_{b,k-2}}{A_0\left(k\right)\left(k-1\right)},\ k \geq 2 \tag{22}$$

The constants $d_{b,0}$ and $d_{a,0}$ can be determined using the boundary conditions, Eqs. (12) and (13), as follows:

$$d_{b,0} = 1$$

and

$$\varepsilon = \sum_{k=0}^{\infty}\left\{\left(\frac{1}{a}-\overline{\psi}\right)(k+1)+\left[1+\overline{\psi}\left(\overline{\theta}-1\right)\right]\right\}d_{a,k} + \left[1+\overline{\psi}\left(\theta-1\right)\right]d_{b,0}+\sum_{k=1}^{\infty}\left\{\left(\frac{1}{a}-\overline{\psi}\right)k+ \left[1+\overline{\psi}\left(\overline{\theta}-1\right)\right]\right\}d_{b,k} \quad (23)$$

Taking Eq. (20) into Eq. (14), one can get the dialysate phases concentration

$$\zeta_D = \left(\frac{1}{a}-\overline{\psi}\xi\right)\left(\sum_{k=0}^{\infty}(k+1)d_{a,k}\xi^k + \sum_{k=1}^{\infty}(k)d_{b,k}\xi^{k-1}\right)+\left[1+\overline{\psi}\left(\overline{\theta}-1\right)\right] \left(\sum_{k=0}^{\infty}d_{a,k}\xi^{k+1}+\sum_{k=0}^{\infty}d_{b,k}\xi^k\right) \quad (24)$$

Hence the outlet concentrations in the retentate and dialysate phases are

$$\zeta_R(1) = \zeta_{R,o} = \sum_{k=0}^{\infty}d_{a.k}+\sum_{k=0}^{\infty}d_{b,k} \quad (25)$$

and

$$\zeta_D(0) = \zeta_{D,o} = \frac{d_{a,0}+d_{b,1}}{a} + \left[1+\overline{\psi}\left(\overline{\theta}-1\right)\right]d_{b,0} \quad (26)$$

respectively.

3. Mass-transfer efficiency improvement

The overall mass transfer rate in a dialyzer can be determined by

$$M = Q_{R,i}C_{R,i}-Q_{R,o}C_{R,o} = Q_{D,o}C_{D,o}-Q_{D,i}C_{D,i} \quad (27)$$

Two expressions of separation efficiency for a dialysis system coupled with ultrafiltration are used in this study. The separation efficiency η is defined as the ratio of the actual mass transfer rate to the maximum possible mass transfer rate by only diffusion:

$$\eta = \frac{M}{LWK\left(C_{R,i}-C_{D,i}\right)} = \frac{1-\left(1-a\overline{\psi}\right)\zeta_{R,o}}{a\left(1-\varepsilon\right)} \quad (28)$$

The term $LWK\ (C_{R,i} - C_{D,i})$ in Eq. (28) is the mass transfer rate while the retentate and dialysate concentrations are kept at their inlet concentrations in a dialysis operation without ultrafiltration. Another definition of separation efficiency, χ, is the ratio of the actual mass transfer rate to the maximum solute mass difference:

$$\chi = \frac{M}{Q_{R,i}\left(C_{R,i}-C_{D,i}\right)} = \frac{1-\left(1-a\overline{\psi}\right)\zeta_{R,o}}{\left(1-\varepsilon\right)} \quad (29)$$

The term $Q_{R,I}(C_{R,i} - C_{D,i})$ in Eq. (29) is the deference of solute amount between the retentate and dialysate flows at the inlet of conduit. The mass-transfer efficiency improvement by employing a dialysis system coupled with ultrafiltration operation is best illustrated by calculating the percentage increase in mass transfer efficiency based on a dialysis system without ultrafiltration

$$E\% = \frac{\eta-\eta_{\psi=0}}{\eta_{\psi=0}}\times 100\% = \frac{\chi-\chi_{\psi=0}}{\chi_{\psi=0}}\times 100\% \quad (30)$$

4. Experiments

An experimental module of the parallel-plate countercurrent dialysis system is shown in Fig. 2. Two channels were formed by inserting a hydrophilic composite membrane (composed of cellulose acetate cast on a thin polypropylene backing materials, Spectrum Laboratories Inc., MWCO = 10,000) into the parallel-plate module. The working dimensions of each channel are L = 18 cm, W = 8.5 cm and H = 0.2 cm. The retentate phase was 2 M urea solution and the dialysate phase was pure water. Two peristaltic pumps were used to pump the retentate and dialysate feed into the top and bottom channels of the parallel-plate module, respectively. The pulsing of the pulsatile flow was reduced by using the small size tubes (4.8 mm inner diameter) and raising the peristaltic pump speed to keep the desired flow rate. The retentate feed flow rates were 20, 25, 30, 35 and 40 cm^3/min and the dialysate feed flow rate was kept at 300 cm^3/min. The ultrafiltration flow rates were 0, 5 and 10 cm^3/min which were regulated by adjusting the valve at the retentate outlet in this study. The feed flow rates of retentate and dialysate were controlled by the flow meters while the outlet flow rates were regulated by the valves at the both ends of the device and recorded by the flow meters which were next to the valves. Moreover, the transmembrane pressure between the retentate and dialysate flow are adjusted by the valves at the inlet and outlet of the retentate and dialysate flows as shown in Fig. 2. The urea outlet concentration in retentate phase was monitored using a UV detector (Unicam UV 300 UV-Visible Spectrometer, Uni-. cam UV/VLS, UK) at the end of the retentate flow at 5 min intervals as shown in Fig. 2. The experimental run was finished until the urea concentration was unchanged (steady state).

5. Results and discussion

The concentration profile of the retentate phase can be determined by Eq. (20) and the calculated results are illustrated in Fig. 3 where the x-axis is the dimensionless conduit length, $\xi = x/L$. The solute concentration of the retentate phase in the conduit is only a function of the conduit and it is not a function of time at steady state as shown in Fig. 3. Due to the fact that the solute is transported from the retentate phase to the dialysate phase, the retentate phase concentration decreases along the conduit. The solute can pass through the membrane freely while $\overline{\theta} = 1$ and it is partially rejected by the membrane while $\overline{\theta} < 1$. Hence, in the case of $\overline{\theta} < 1$ the solute concentration decreases slowly along the conduit for high $\overline{\psi}$ but, in the case of $\overline{\theta} = 1$, it decreases quicker along the conduit for high $\overline{\psi}$. Figs. 4 and 5 show the retentate phase outlet concentrations, $\zeta_{R,o}$, vs.a with ψ and b as parameters, respectively. As can be observed from Fig. 4, the retentate outlet concentration decreases with increasing a (decreasing retentate-phase flow

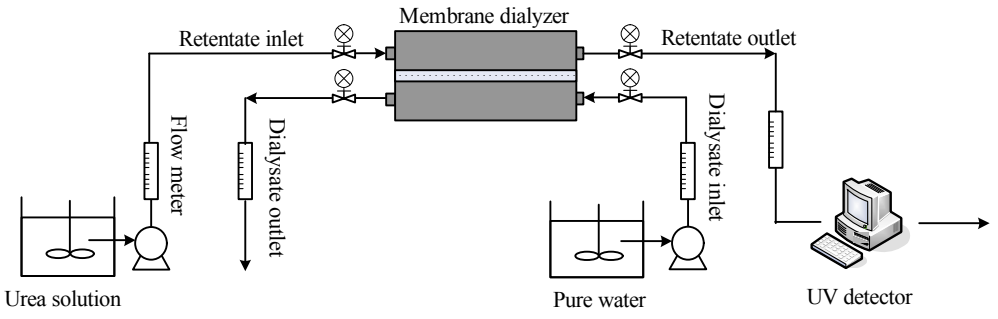

Fig. 2. Experimental module of the parallel-plate countercurrent dialysis system.

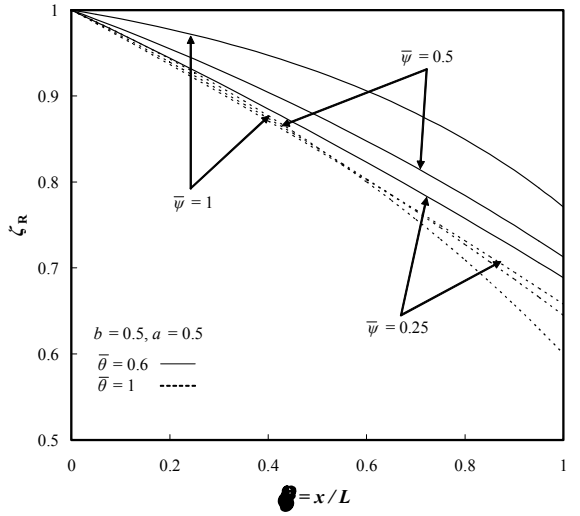

Fig. 3. Retantate-phase concentration along the conduit with ψ as a parameter; a = 0.5, b = 0.5, θ = 1 and 0.6.

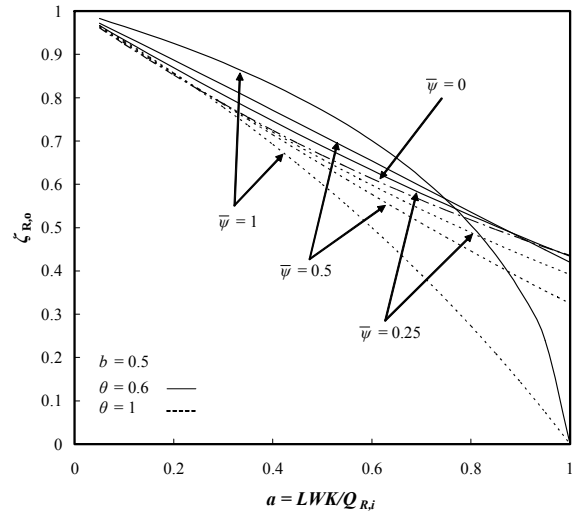

Fig. 4. Outlet concentration of retantate phase vs. a with ψ as a parameter; b = 0.5, θ = 1 and 0.6.

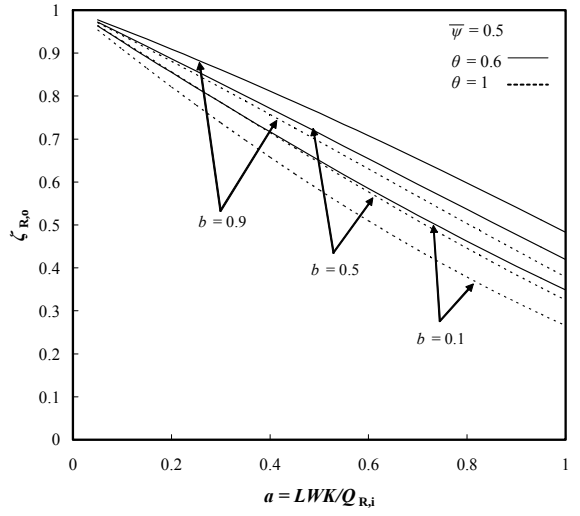

Fig. 5. Outlet concentration of retantate phase vs. a with b as a parameter; ψ = 0.5, θ = 1 and 0.6.

rate). This can be attributed to the increase of the residence time of the solute in the module with decreasing the retentate-phase flow rate. The line of $\overline{\psi}$ in Fig. 4 denotes the retentate outlet concentration of the pure dialysis system. As indicated in Fig. 4, the retentate outlet concentration in the dialysis-and-ultrafiltration system is lower than that in the pure dialysis system for large a, especially for $\overline{\theta}$ = 1. The effects of the dimensionless dialysate-phase flow rate, b, are shown in Fig. 5. The retentate outlet concentration, $\zeta_{R,o}$, decreases with decreasing b. This is because the higher dialysate-phase flow rate results in larger concentration differences between the retantate and dialysate phases and hence, more solute can be transported from the retentate phase to the dialysate phase.

The theoretical predictions of the separation efficiency, η, are determined by Eq. (28) and the results are shown in Figs. 6 and 7 with ψ and b as the parameters, respectively. Because of the separation efficiency, η, is based on the maximum possible mass transfer rate by diffusion, the influence of ultrafiltration operation on the mass transfer is lower while the lower retentate-phase flow rate (higher a) or higher dialysate-phase flow rate (lower b) is operated. The mass transfer rate of the solute can be influenced by the resident time of fluid in the conduit and the force convection

mass transfer coefficient of the fluid in a counter-current mass transfer system. Therefore, while the increase in the retentate flow rate, the difference of the retentate inlet and outlet concentration, $C_{R,i} - C_{R,o}$, will decrease due to the shorter resident time. However, with respect to the definition of the mass transfer rate in this study as shown in Eq. (27), $M = Q_{R,i}C_{R,i} - Q_{R,o}C_{R,o} = Q_{D,o} - Q_{D,i}C_{D,i}$, the total amount of the solute transferred from the retentate phase to the dialysate phase increases due to the increase of the force convection mass transfer coefficient with increasing the retentate phase flow and this effect can compensate the decrement of the mass transfer time in the retentate phase. Hence, for a fixed dialysate flow rate, the outlet concentration of dialysate $C_{D,o}$ and the mass transfer rate defined in Eq. (27) increase with increasing the retentate flow rate. Hence the separation efficiency η increases with decreasing *a* and *b*, as indicated in Figs. 6 and 7 respectively. Moreover, Fig. 6 also shows that the separation efficiency η increases with increasing $\overline{\psi}$. The values of η > 1 in Figs. 6 and 7 indicate that ultrafiltration operation in a dialysis system can readily enhance the mass transfer rate. The second separation efficiency χ is based on the maximum solute concentration difference in two phases, as shown in Eq. (29) and the calculating results are illustrated in Figs. 8 and 9. The residence time of the fluid increases with decreasing *a* resulting in that the solute has enough time to transfer to the dialysate phase. Hence, the separation efficiency χ increases with increasing *a* (i.e. decreasing retentate-phase flow rate) as shown in Figs. 8 and 9. Moreover, the effects of the dialysate-phase flow rate, ultrafiltration flux and membrane sieving coefficient on the separation efficiency χ are the same as those on the separation efficiency η as represented in Figs. 8 and 9.

The mass-transfer efficiency improvement of the dialysis system coupled with ultrafiltration was defined as the increasing percentage in the separation efficiency η (or the separation efficiency χ) based on that of the pure dialysis module. As illustrated in Fig. 10, the mass-transfer efficiency improvement *E*(%) increases with increasing ultrafiltration flux and average membrane sieve coefficient. Fig. 11 indicates that the mass-trans-

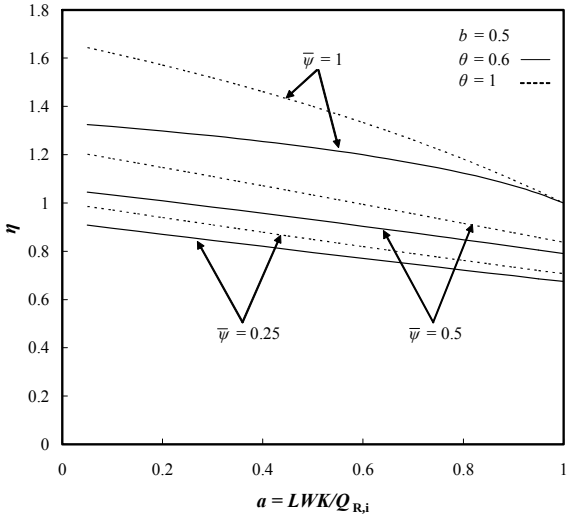

Fig. 6. Separation efficiency η vs. *a* with ψ as parameters; *b* = 0.5, θ = 1 and 0.6.

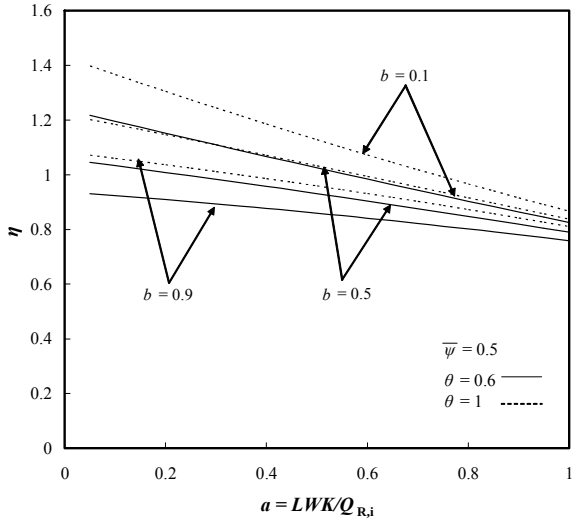

Fig. 7. Separation efficiency η vs. *a* with *b* as parameters; ψ = 0.5, θ = 1 and 0.6.

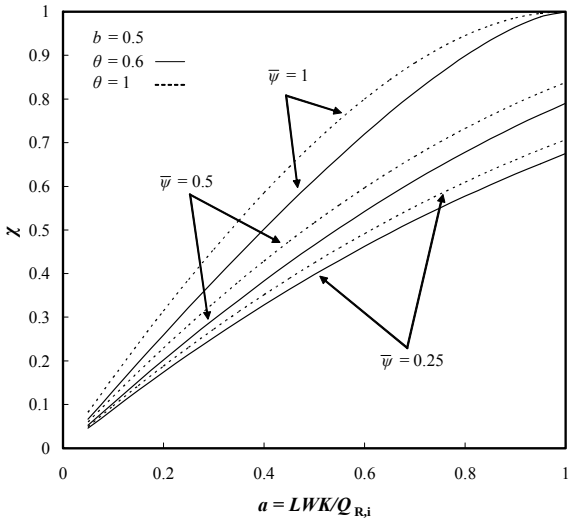

Fig. 8. Separation efficiency χ vs. *a* with ψ as parameters; *b* = 0.5, θ = 1 and 0.6.

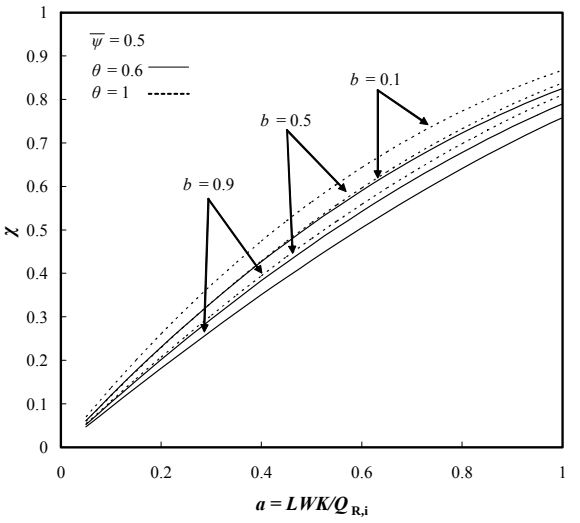

Fig. 9. Separation efficiency χ vs. *a* with *b* as parameters; ψ = 0.5, θ = 1 and 0.6.

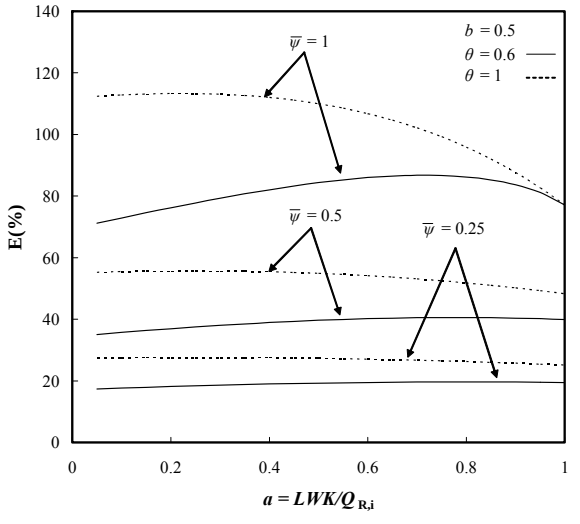

Fig. 10. Mass transfer improvement *E*(%) vs. *a* with ψ as parameters; *b* = 0.5, θ = 1 and 0.6.

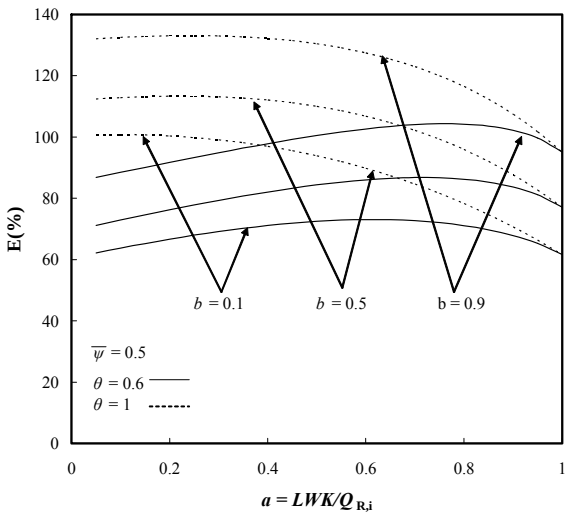

Fig. 11. Mass transfer improvement *E*(%) vs. *a* with *b* as parameters; ψ = 0.5, θ = 1 and 0.6.

fer efficiency improvement *E*(%) increases with increasing *b* (decreasing dialysate-phase flow rate). It can be attributed to the solute concentration difference between the retentate and dialysate phases increasing with increasing *b* resulting in that the mass transfer in diffusion (caused by the concentration difference) is more comparable to that in convection (caused by ultrafiltration). Hence, the effects of ultrafiltration flux are slight in the case of a high dialysate-phase flow rate.

Fig. 11 also shows that the mass-transfer efficiency improvement $E(\%)$ decreases with increasing a for $\bar{\theta} = 1$. While in the case of $\bar{\theta} = 0.6$, the optimal values of mass-transfer efficiency improvement exist in the specific retentate-phase flow rate at $a = 0.65$ and $b = 0.1$, and $a = 0.8$ at $b = 0.5$ and 0.9, respectively.

An experiment of counterflow parallel-plate membrane dialysis module was setup to confirm the accuracy of the mathematical model. Due to the fact that high efficiency hemodialyzer is usually defined by a high clearance rate of urea [30], urea was selected as the solute in the experiment. The dialysate feed flow rate was kept at 300 cm^3/min, and the retentate feed flow rate was controlled between 20 and 40 cm^3/min. The ultrafiltration flow rates Q_m were controlled as 0 cm^3/min, 5 cm^3/min and 10 cm^3/min in the experimental runs and the corresponding ultrafiltration fluxes, calculated by $\bar{V}_m = Q_m/WL$, were $\bar{V}_m$ = 0 cm/min, 0.0327 cm/min and 0.0654 cm/min, respectively, based on the membrane area 153 cm^2. The dimensionless values of the retentate feed flow rate, ultrafiltration flux, and dialysate feed flow rate were $a = 0.039$–0.078, $\bar{\psi} = 0$–6.4 and $b = 0.0052$. The average overall mass transfer coefficient K was estimated by the experimental retentate outlet concentrations. The estimating procedure of the average overall mass transfer coefficient K in the present study is as follows. Firstly, by assuming a value of K with the corresponding values of a, b and $\bar{\psi}$ and substituting these values into Eq. (25), a theoretical outlet concentration of the retentate phase, $C_{R,o}^{\text{Theo}}$, can be obtained. For each experimental run, one can find the error of the theoretical prediction, $C_{R,o}^{\text{Theo}} - C_{R,o}^{\text{Exp}}$, where $C_{R,o}^{\text{Exp}}$ is the experimental outlet concentration of the retentate phase. The best estimation value of K was obtained with the least squares of the theoretical prediction errors, say

$$\sum\left(C_{R,o}^{\text{Theo}} - C_{R,o}^{\text{Exp}}\right)^2 .$$

The percentage error of the theoretical prediction is defined as

$$\text{Err}(\%) = \frac{\left(C_{R,o}^{\text{Theo}} - C_{R,o}^{\text{Exp}}\right)}{C_{R,o}^{\text{Exp}}} \times 100\% \tag{31}$$

and the calculated results are shown in Table 1. Because the average overall mass transfer coefficient of solute $K = 0.0102$ cm/min is chosen in this study, the theoretical prediction errors ($C_{R,o}^{\text{Theo}} - C_{R,o}^{\text{Exp}}$) will not be zero. Actually, the overall mass transfer coefficient of solute K will increase with increasing the ultrafitration flow rate Q_m. Hence the percentage errors of the theoretical prediction are positive for $Q_m = 0$ cm^3/min and negative for $Q_m = 10$ cm^3/min, respectively, as shown in Table 1, and also the maximum percentage error is –5.68% when the experimental run operated at $Q_{R,i} = 20$ cm^3/min and $Q_m = 10$ cm^3/min. The results in Table 1 show that the present theoretical model is reliable.

The overall mass transfer coefficient of solute K is influenced by the retantate flow rate $Q_{R,i}$ and ultrafitration flow rate Q_m. However, in order to simplify the problem, an average value of the overall mass transfer coefficient of the solute K within the range of $Q_{R,\text{i}} = 20$–40 cm^3/min and $Q_m = 0$–10 cm^3/min was used in this study. Under the presented experimental operating conditions, the correlating results show that the average overall urea mass transfer coefficient is $K = 0.0102$ cm/min in this work. Moreover, because the particle size is directly proportional to its molecular weight and the MWCO of the hydrophilic composite membrane is MWCO = 10,000 which is much larger than the molecular weight of urea MW = 60.06, the sieving factor $\bar{\theta}$ of urea is to be expected as $\bar{\theta} = 1$ in this study. The experimental mass transfer rates of the solute are illustrated in Fig. 12. Due to the fact that urea can freely pass through the hydrophilic composite membrane using in the experiment and no urea will accumulate on the membrane, the osmotic pressure effect on the mass transfer can be ignored in the present work. A small amount of solvent would unavoidably pass through the membrane while the

Table 1
The comparisons of the experimental and theoretical results of the outlet concentration in retentate phase for $Q_{D,i}$ = 300 cm^3/min.

$Q_{R,i}$ (ml/min)	$C_{R,o}$ (mol/L)								
	Q_m = 0 cm^3/min			Q_m = 5 cm^3/min			Q_m = 10 cm^3/min		
	Exp.	Theo.	Err.(%)	Exp.	Theo.	Err.(%)	Exp.	Theo.	Err.(%)
20	0.898	0.925	3.00	0.922	0.915	–0.79	0.953	0.899	–5.68
25	0.912	0.940	3.07	0.931	0.933	–0.24	0.957	0.925	–3.36
30	0.925	0.949	2.66	0.948	0.945	–0.32	0.964	0.940	–2.49
35	0.940	0.957	1.81	0.957	0.954	–0.38	0.970	0.950	–2.13
40	0.944	0.962	1.93	0.962	0.960	–0.27	0.977	0.957	–2.04

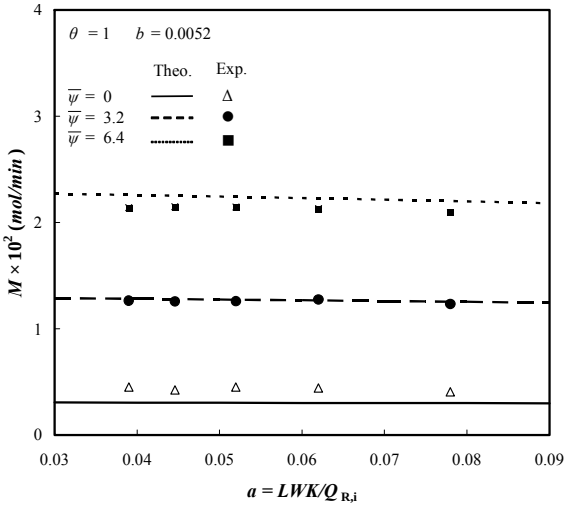

Fig. 12. Experimental and theoretical results of mass transfer rate *M*.

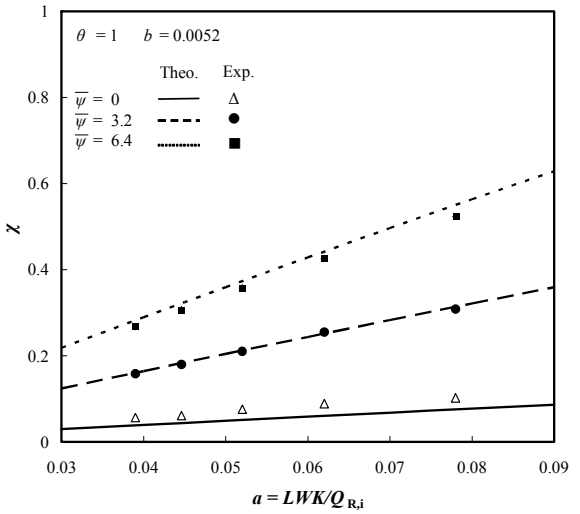

Fig. 13. Experimental and theoretical results of separation efficiency χ.

pure dialysis condition was operated in the experimental runs. Hence the larger errors between the theoretical and experimental results occur at the pure dialysis operation runs, i.e. $\bar{\psi}$ = 0, as shown in Fig. 12. The experimental and theoretical separation efficiency results χ are shown in Fig. 13. It is evident that the theoretical model developed in this study shows good agreement with the experimental data, as observed from the results in Figs. 12 and 13.

6. Conclusions

A mathematical model of a parallel-plate countercurrent dialysis system was developed in this study. In a dialysis-and-ultrafiltration system, the solute is transported in two ways: diffusion (caused by the concentration different in two phases) and convention (caused by ultrafiltration). The theoretical results show that the mass transfer rate increases with increasing ultrafiltration

flux, membrane sieving coefficient, retentate-phase flow rate and dialysate-phase flow rate. As demonstrated in Figs. 10 and 11, the mass-transfer efficiency of the parallel-plate countercurrent membrane dialyser can be improved by applying ultrafiltration in a dialysis system. The experiment was conducted to check the accuracy of the theoretical prediction results. The results in Figs. 12 and 13 show that the theoretical results are in good agreement with the experimental data. Hence the mathematical model developed in this study is reliable. Instead of the hollow fiber system, a parallel membrane-sheet dialysis system was studied in the present work due to one dialysate stream with one retentate stream was expected to confirm the adequacy of the theoretical mathematical model. Moreover, the present mathematical model can be extended to simulate a hollow fiber dialysis system by only changing the symbol W to $2N\pi r$ in the model equations by assuming no interaction among all fibers, in which N is the number of fibers and r is the fiber radius. Therefore, the values of the present work are to develop a simple one-dimension mathematical model and predict the mass transfer rate of the parallel-plate membrane or hollow fiber dialysis systems with or without ultrafiltration operation.

Acknowledgement

The authors wish to express their sincere gratitude to the National Science Council (NSC), the Center of Excellence (COE) Program on Membrane Technology from the Ministry of Education (MOE), ROC, and the Technology Development Program for Academia (TDPA) from the Ministry of Economic Affairs (MOEA), ROC, for the financial support.

Symbols

A_0, A_1, A_2 — Calculating coefficient defined in Eq. (17)
A — Flow rate in the retentate phase
a — Retentate-phase flow rate
B_0, B_1 — Calculating coefficient defined in Eq. (17)
B — Flow rate in the dialysate phase
b — Dialysate-phase flow rate
C — Solute concentration, mol/cm^3
C_0 — Calculating coefficien, defined in Eq. (17)
E — Mass transfer improvement defined in Eq. (30)
Err. — Percentage error of theoretical prediction defined in Eq. (31)
d_{ak}, d_{bk} — Expansion coefficients defined in Eq. (20).
H — Conduit height, cm
K — Overall mass transfer coefficient of solute, cm/min
L — Conduit length, cm
M — Mass transfer rate, mol/min
N — Number of fibers
Q — Volumetric flow rate, cm^3/min
Q_m — Ultrafiltration flow rate, cm^3/min
r — Fiber radius, cm
V_m — Ultrafiltration flux, cm/min
$\bar{V}_m$ — Average ultrafiltration flux, cm/min
W — Conduit width, cm
x — Axial coordinate, cm

Greek

χ — Separation efficiency defined in Eq. (25)
ε — Ratio of inlet solute concentration in dialysate phase to that in the retentate phase, $C_{D,i}/C_{R,i}$
η — Separation efficiency defined in Eq. (23)
λ — Coefficient of the power series in Eq. (19)
$\bar{\theta}$ — Average membrane sieving coefficient
ξ — Coordinate, x/L
ψ — Ultrafiltration flux, V_m/K
$\bar{\psi}$ — Average dimensionless ultrafiltration flux, $\bar{V}_m / K$

ζ — Solute concentration

Superscripts and subscripts

D — Dialysate phase
Exp — Experimental data
i — Inlet
o — Outlet
R — Retentate phase
Theo — Theoretical results

References

[1] M. Mulder, ed., Basic Principles of Membrane Technology, Kluwer Academic Publishers, London, 1997.
[2] M. Vajda, I. Havalda and R. Macek, Membrane-based solvent extraction and stripping of zinc in a hollow-fibre contactor operating in a circulating mode, Desalination, 163 (2004) 19–25.
[3] H.M. Yeh, C.H. Chen and T.Y. Yueh, Influence of channel-width ratio on solvent extraction through a double-pass parallel-plate membrane module, J. Membr. Sci., 230 (2004) 13–19.
[4] I. Ortiz, E. Bringas, M.F. San Román and A.M. Urtiaga, Selective separation of zinc and iron from spent pickling solutions by membrane-based solvent extraction: Process viability, Sep. Sci. Tech., 39 (2004) 2441–2455.
[5] P.S. Kumar, J.A. Hogendoorn, P.H.M. Feron and G.F. Versteeg, New absorption liquids for the removal of CO_2 from dilute gas streams using membrane contactors, Chem. Eng. Sci., 57 (2002) 1639–1651.
[6] W.P. Wang, S.T. Lin and C.D. Ho, An analytical study of laminar co-current flow gas absorption through a parallel-plate gas–liquid membrane contactor, J. Membr. Sci., 278 (2006) 181–189.
[7] H.K. Lee, H.D. Jo, W.K. Choi, H.H. Park, C.W. Lim and Y.T. Lee, Absorption of SO_2 in hollow fiber membrane contactors using various aqueous absorbents, Desalination, 200 (2006) 604–605.
[8] N.P. Gnusin, N.P. Berezina, N.A. Kononenko and O.A. Dyomina, Transport structural parameters to characterize ion exchange membranes, J. Membr. Sci., 243 (2004) 301–310.
[9] Y. Tanaka, Concentration polarization in ion-exchange membrane electrodialysis: The events arising in an unforced flowing solution in a desalting cell, J. Membr. Sci., 244 (2004) 1–16.
[10] V.V. Ugrozov, I.B. Elkina, V.N. Nikulin and L.I. Kataeva, Theoretical and experimental research of liquid-gap membrane distillation process in membrane module, Desalination, 157 (2003) 325–331.
[11] A.M. Alklaibi and N. Lior, Transport analysis of air-gap membrane distillation, J. Membr. Sci., 255 (2005) 239–253.
[12] E. Klein, E.F. Holland, A. Lebeouf, A. Donnand and J.K. Smith, Transport and mechanical properties of hemodialysis hollow fibers, J. Membr. Sci., 1 (1976) 371–396.
[13] W.S.W. Ho and K.K. Sirkar, Membrane Handbook, Van Nostrand Reinhold., New York, 1992.
[14] L. Grimsurd and A.L. Babb, Velocity and concentration profiles for laminar flow of Newtonian fluid in a dilyzer, Chem. Eng. Prog. Symp. Ser., 62 (1966) 20.
[15] C.K. Colton, K.A. Smith, P. Stroeve and E.W. Merrill, Laminar flow mass transfer in a flat duct with permeable walls, AIChE J., 17 (1971) 773–780.
[16] G. Walker and T. Davis, Mass transfer in laminar flow between parallel permeable plates, AIChE J., 20 (1974) 881–889.
[17] D.O. Cooney, S.S. Kim and E.J. Davis, Analyses of mass transfer in hemodialyzers for laminar blood flow and homogeneous dialysate, Chem. Eng. Sci., 29 (1974) 1731–1738.
[18] I. Noda and C.C. Gryte, Mass transfer in regular arrays of hollow fibers in countercurrent dialysis, AIChE J., 25 (1979) 113–122.
[19] C. Gostoli and A. Gatta, Mass transfer in a hollow fiber dialyzer, J. Membr. Sci., 6 (1980) 133–148.
[20] R. Popovich, G. Christopher and A.L. Babb, The effect of membrane diffusion and ultrafiltration properties on hemodialyzer design and performance, Chem. Eng. Prog. Symp. Ser., 67 (1971) 105.
[21] L.W. Henderson, Current status of hemofiltration, Artif. Organs, 2 (1978) 120.
[22] H.W. Leber, V. Wizemann, G. Goubeaud, P. Rawer and G. Schutterle, Hemodiafiltration: a new alternative to hemofiltration and convectional hemodialysis, Artif. Organs, 2 (1978) 150.
[23] R. Jagannathan and U.R. Shettigar, Analysis of a tubular haemodialyser-effect of ultrafiltration and dialysate concentration, Med. Biol Eng. Comput., 15 (1977) 500–512.
[24] M. Abbas and V.P. Tyagi, Analysis of a hollow-fiber artificial kidney performing simultaneous dialysis and ultrafiltration, Chem. Eng. Sci., 42(1) (1987) 133–142.

[25] M. Abbas and V.P. Tyagi, On the mass transfer in a circular conduit dialyzer when ultrafiltration is coupled with dialysis, Int. J. Heat Mass Transfer, 31(3) (1988) 591–602.
[26] H.M. Yeh, T.W. Cheng and Y.C. Chen, Analysis of dialysis coupled with ultrafiltration in cross-flow membrane modules, J. Membr. Sci., 134 (1997) 151–162.
[27] H.M. Yeh, T.W. Chen and Y.J. Chen, Mass transfer for dialysis with ultrafiltration flux declined in cross-flow membrane modules, J. Chem. Eng. Jpn., 33 (2000) 440.
[28] C. Legallais, G. Catapano, B. Harten and U. Baurmeister, A theoretical model to predict the in vitro performance of hemodialfilters, J. Membr. Sci., 168 (2000) 3.
[29] M.Y. Jaffrin, L. Ding and J.M. Laurent, Simultaneous convective and diffusive mass transfers in a hemodialyzer, J. Biomech. Eng., 112 (1990) 212.
[30] J. Levy, J. Morgan and E. Brown, Oxford Handbook of Dialysis, Oxford University Press, UK, 2004.